CORROSION INDUCED BY CO_2 AND H_2S SATURATED STEAM CONDENSATES IN THE UPPER MAHIAO PIPELINE, LEYTE, PHILIPPINES

Ruperto R Villa, Jr.

PNOC Energy Development Corporation, Merritt Road, Ft. Bonifacio, 1201 Makati City, Philippines

ABSTRACT

A polarization experiment using different types of metal coupons immersed in the Upper Mahiao condensate was conducted to elucidate the processes that control corrosion. Results showed that low carbon steel is incapable of forming a protective layer because of the continued breakdown of the protective film. Austenitic stainless steel showed a very wide range of passivation zone, suggesting that it is very resistant to this type of fluid acidity.

From analytical methods such as SEM, EPMA, XRD and XR-Fluorescence were conducted on the corrosion samples to determine the actual chemical composition and the morphology of the corrosion products. The contrasting effect of high temperature steam and low temperature condensate to the steel facilitated hydrogen infusion which promotes blistering and sulfide corrosion at the first and second stages of the turbine that breaks down the protective film into secondary corrosion products at low temperature durmg shutdowns. This leads to the exposure of deeper steel material to acidic environment. This condition coupled with the erosive velocity of the fluid along these stages, resulted to wearing of the turbine parts. The polarization of ordinary martensitic steel (12%Cr) suggests that it is not reliably resistant to corrosion using the above fluid. Thus, a more appropriate material (i.e. martensitic steel with higher %Cr, %Mo and or %Ni) is needed for the turbine.

1.0 INTRODUCTION

In December 1997, the Geothermal Combined Cycle Power Plant was commissioned in the Upper Mahiao sector of the Tongonan Geothermal Field, Leyte, Philippines. It has a net plant capacity of 125 MW, considered as the world's largest power plant with vast network of air-cooled non-contact cooling tower (Ormat, 1998). At full load, the power plant produces a total of 270 kg/s steam condensates obtained from the heat-exchange system. These condensates are saturated with dissolved CO_2 and H_2S gases that promoted acid attack on the condensate pipelines barely three months from the start of operation. To deal with the problem of condensate pipeline corrosion, two field material tests were conducted at Upper Mahiao to identify the appropriate material that can withstand the corrosive nature of the condensates. Although both tests showed that low carbon steel is not resistant to this type of fluid, it did not clearly explain the corrosion mechanism in the pipeline.

Thus, a polarization experiment was conducted at Kyushu University Material Science Laboratory to shed light on the Corrosion mechanism involved. Moreover, an extensive analysis of the corrosion samples using Scanning Electron Microscope (SEM), Electron Robe Micrograph Analysis (EPMA), X-Ray Diffraction (XRD) and X-Ray Fluorescence Analysis was conducted at the Kyudensangyo Industries Laboratory to identify the corrosion processes and corrosion product morphology.

2.0 POWER PLANT PROCESS FLOW AND CONDENSATE DISPOSAL

The power plant operation is based on Geothermal Combined Cycle Units (GCCU). The unit is a combination of a back pressure steam turbine generator (STG) operating at high pressure and at around 180~188°C followed downstream by sets of Ormat Energy Converters (OEC) systems operating on an Organic Rankine Cycle (Forte, 1996). These OEC's basically consist of shell-and-tube heat exchanger which vaporize the organic binary fluid (n-pentane) to drive the attached low-pressure turbine. A simplified process flow of this power plant is presented in Figure 1. From the OEC heat exchangers, the fully condensed steam is separated fiom the Non-Condensable Gases

(NCG) at a temperature between 50-60°C. While the NCG is treated in the Abatement Plant prior to its dispersal to the atmosphere, all the condensates are piped downstream in a low carbon steel pipeline towards the spray tower (Figure 2). The temperature drops further at the spray tower to meet the environmental guidelines prior to mixing with river.

Although the Non-Condensable Gases (NCG) were separated fiom the condensates, it is still saturated with CO_2 and H_2S gases after separation **fiom** the OEC as shown by its typical chemistry listed in Table 1. These gases are believed to be those that control acidity and the primary factors that promote corrosion attack (Salonga et al., 1998). During the first three months of Upper Mahiao power plant operation (December 1996 to March 1997), problems were already encountered at the condensates pipeline. The downstream spray tower nozzles were usually clogged with black solid particle containing FeS_2 and Fe_2O_3. Line maintenance required diverting the flow using a separate alvenius pipeline to facilitate declogging.of the nozzles (Figure 2). **Three** (3) months later on March 1997, **a** long crack (around 2 meters) was observed at the bottom part of the pipe causing severe leakage (Villa, 1997). Radiographic and ultrasonic testing revealed that severe pipe thinning at the bottom of the pipe.

This event triggered the conduct of material testing to identify the material suitable for its long-term utilization (Salonga **et** al., 1997). Given the acidic nature of condensates, long term disposal is uncertain **since** there is a risk of reinjection pipeline and borehole corrosion.

3.0 SUMMARY OF FIELD MATERIAL TESTING

The material consisted of two parts. The first testing was conducted on July to September 1997 along the main steam lines and the other was conducted (March to May 1998) at the condensates line.

The first experiment confirmed that stainless 304 and 316 are resistant to the condensates-induced corrosion. The other materials tested (low carbon steel and drill pipe) are not resistant, except, for the alvenius pipes which showed a relative resistance in areas where its **galvanized** coatings were intact. The second experiment affirmed the conclusions of the first experiment. Moreover, it has the following additional finding:

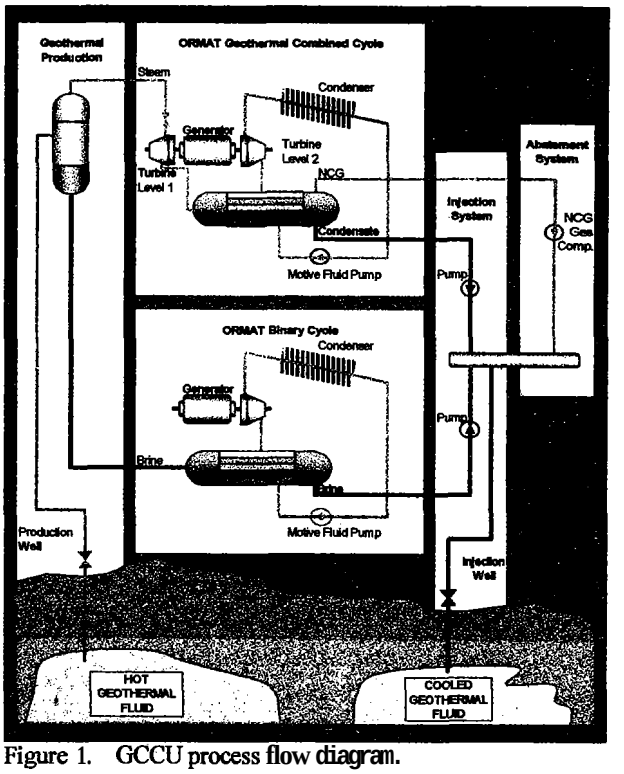

Figure 1. GCCU process flow diagram.

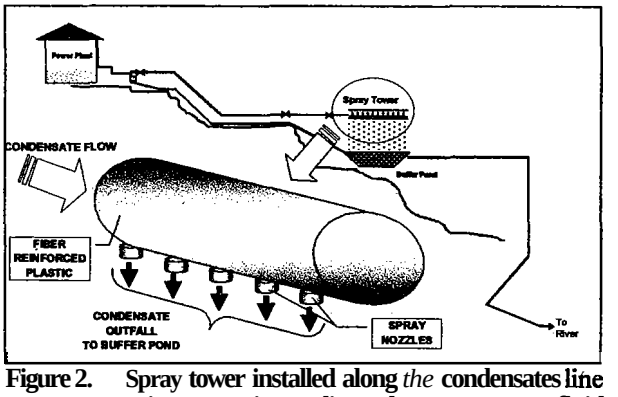

Figure 2. Spray tower installed along *the* condensates line prior to river disposal to reduce fluid temperature.

Table 1. Ranges of different dissolved chemical constituents of Upper Mahiao condensates. Note that other heavy metal components such as Hg, Cd, Cr and Co co-exist in trace amounts.

Component	Range, ppm	Component	Range, ppm
pH	5.2-5.9	Cl	3.7-4.4
Na	0.3-3.6	B	3.6-4.4
K	0.1-2.0	HCO_3	16.9-183.0
Fe	0.8-4.0	CO_2	67.2-240.7
As	0.02-0.04	H_2S	2.0-14.5
TDS	4.9-14.3	NH_3	11.9-13.2
SiO_2	<0.01-0.26	D.O, ppm	0.04-0.12

(1) the condensates are largely composed of dissolved CO_2 gas with significant amount of H_2S and NH_3;
(2) dissolved sulk exists as H_2S at lower oxidation potential (Eh) and as SO_4 at higher Eh. Native sulfur is expected to form when there is a shift in Eh;
(3) the fluids will favor the formation of free corrosion products of Fe^{++}, and thus, uniform corrosion will always occur (Figure 3). Pyrite is the most probable passive film that will form and hematite will form simultaneously or as a secondary product of pyrite at high Eh environment;
(4) less resistant coupons are affected by uniform and pitting corrosion (Salonga et al, 1998). Given the standard acceptable corrosion rate of 0.2 mm/yr., this suggests that alvenius pipe, low carbon steels and drill pipe corrosion rates >0.2 mm/yr. are not appropriate materials. Only SS-304 and SS-316 (rate >0.20 mm/yr.) are appropriate. Using this material will have no danger in chloride, sulfide or stress corrosion cracking since its operation is only limited to 60°C.

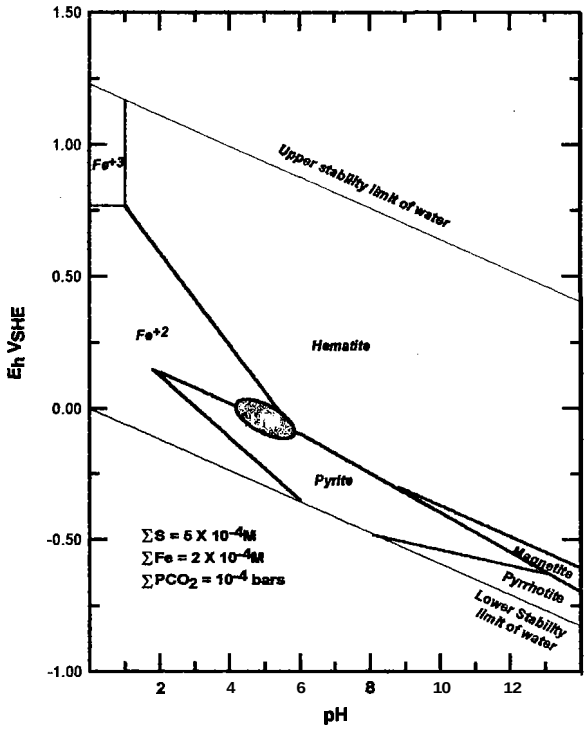

Figure 3. UM Potential-pH (Pourbaix) diagram

4.0 ANALYSES OF PIPELINE CORROSION SAMPLES

The surface SEM morphology of the low carbon steel pipeline corrosion samples showed a rough formation dominated mainly by Fe and S components (Table 2). The EPMA and XRF results showed that Si (as SiO_2) and Ca are almost negligible. Moreover, the cross-sectional structure of these samples from the SEM showed a distinct layer of corrosion.

The lower portion showed a fine-grained layer while the upper portion showed a grainy (hexagonal and tetrahedral) layers which are soft and brittle. Based on XRD analysis, the upper layer is that of $FeSO_4.H_2O$ while the lower layer are that of FeS_2. These products confirm two possible reactions taking place inside the pipeline. The first reaction is the uniform corrosion brought by sulfide and iron reaction forming the pyrite layer. The second reaction is a secondary reaction of pyrite, steel and H_2S with water and probably with atmospheric oxygen forming $FeSO_4.H_2O$. The encrustation of the atmospheric oxygen while it is either on-line or on shutdown was proven to be occurring from these samples. This worsens the corrosion problem. As this reaction progresses, the low carbon steel pipeline will never have a chance to form a protective layer to prevent the further advancement of corrosion.

Table 2. Results of X-Ray Fluorescence and X-Ray Diffraction (XRD) Crystallography.

Sample Name		Low Carbon Steel Pipeline Corrosion	
Item Analyzed		X-Ray Fluorescence	
% Composition	Fe (as Fe_2O_3)	24.13*	(34.50)**
	Cu (as CuO)	0.05	(0.06)
	Ni (as NiO)	<0.02	( )
	Zn (as ZnO)	0.05	(0.06)
	Al (as Al_2O_3)	0.45	(0.84)
	Si (as SiO_2)	5.59	(11.95)
	Mg (MgO)	<0.02	( )
	Pb (as PbO)	<0.02	( )
	Mn (as MnO_2)	<0.02	( )
	Mo (as MoO_3)	<0.02	( )
	Cr (as Cr_2O_3)	<0.02	( )
	Na (Na_2O)	0.96	(1.30)
	Ca (as CaO)	0.17	(0.23)
	Ti (as TiO_2)	<0.02	O
	V (V_2O_5)	<0.02	( )
	S (as SO_3)	24.26	(60.57)
	K (as K_2O)	<0.02	( )
	P (as P_2O_5)	0.13	(0.30)
	Sn (as SnO_2)	<0.02	( )
	W (as WO_3)	0.03	(0.04)
	Nb (as Nb_2O_5)	<0.02	( )
	Total		(109.85)
X-Ray Diffraction Crystal Structure Analysis		FeS_2	
		$FeSO_4.H_2O$	
* element value		** oxide value	

The analysis also showed the contrasting effect of high and low temperature steam and condensate to the steel which facilitated hydrogen infusion into the steel material. This hydrogen infusion promotes blistering and sulfide corrosion. The breakdown of the protective film into a secondary corrosion products at low temperature during shutdowns leads to the exposure of new steel material to acidic environment.

Since geothermal stem is always contaminated with gaseous impurities such as H_2S and CO_2, these impurities are often the cause of corrosion. To overcome this problem requires a prudent design and a careful selection of appropriate materials. However, in the design of geothermal power plants, there is no standard approach as to what material is to be used since geothermal steam quality differs fiom field to field. Every geothermal power plant therefore is unique. This is the reason why geothermal power engineering is called an empirical engineering. Foremost in the design precaution is to avoid rotor and blade failure because of the catastrophic nature when this high-speed, stress-prone rotary component fails. As a standard consideration, only low-strength carbon and alloy steel are acceptable in this component to avoid stress corrosion cracking. Since SUS-304, SUS-316 and other austenitic stainless steel are high strength alloys, they are not suitable for high temperature application due to their susceptibility to stress corrosion cracking specially when used in an environment with high H_2S. Martensitic stainless steel or other high performance steel such as titanium alloys are suitable for this application. But titanium alloys and other high performance steels are usually expensive, and therefore, not economically practical to use. Therefore, only resistant martensitic alloy steels are the practical answer to this need.

5.0 CORROSION ASSESSMENT BY POLARIZATION AT LOW AND HIGH TEMPERATURES

Because majority of corrosion failures are usually electrochemical in nature, it follows therefore that in most of these cases, the corrosion mechanism can be elucidated by electrochemical means through polarization (Romanov, 1969). Based on the processes involved in the Upper Mahiao operation, it is more likely that the corrosion mechanism can be explained by this method. When a current flows into a galvanic cell, for example, the anode becomes more cathodic in potential and the cathode becomes more anodic, the difference of potential becomes smaller. The extent of potential change caused by net current to or from an electrode is called polarization (Uhlig, 1967).

Measuring and recording of the polarization data during the corrosion experiment is important because of the following reasons: (1) to study the kinetics of the cathodic or anodic processes; (2) to determine the optimum protective current if cathodic or other protection is to be applied; (3) to determine the differential effects graphically; (4) to investigate the influence of cathodic contacts on the corrosion of constructi'on materials; and (5) to investigate passivation.

In practice also, polarization curves are often plotted to elucidate the influence of some factors on the corrosion rate. These factors usually influence certain stage of the cathodic and anodic processes. The degree to which any stage of the anodic or cathodic processes is inhibited is characterized by the degree to which the potential is increased or decreased by the slope of polarization curves. Consequently, from the slopes of the curves it is possible to determine not only the type of the process being investigated but also which fundamental reactions governing these processes are influenced by a given factor.

Figure 4 is the schematic presentation of the processes involved in the ideal cathodic polarization curve. The graph has threecharacteristicsections: (1) activation; (2) passivation; and (3) hydrogen evolution. Activation is the cathodic depolarization at the corresponding corrosion current and potential which is due to the reduction of oxygen on the local

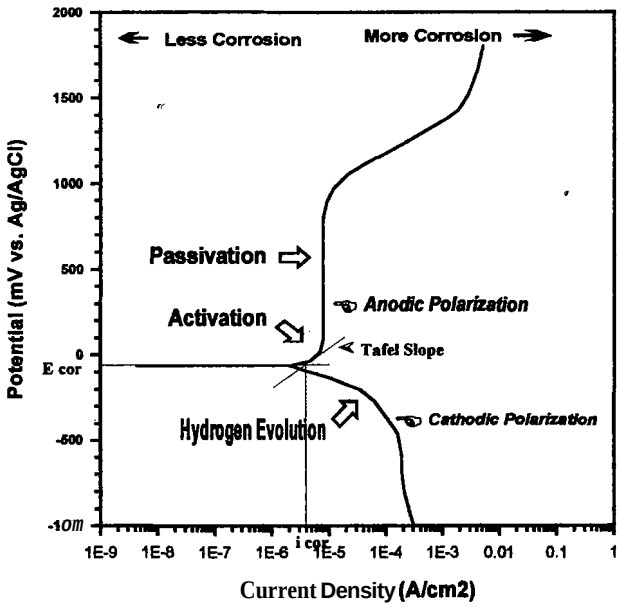

Figure 4. Ideal polarization curve.

microcathodes. On the other hand, the shape of passivation curve is determined by inhibition of the diffusion of oxygen to the microcathodes. The hydrogen evolution curve represents corrosion currents and potential at which the cathodic process is caused by evolution of hydrogen fiom the test media. The degree of the extent of corrosion can be estimated based on the amount of current density it absorbed at specific potential. Figure 5 shows the polarization curves of different metal coupons tested (compositions are listed in Table 3) using the Upper Mahiao condensate (Table 4) and Ag/AgCl as standard electrode. As observed, low carbon steel (IF) corrosion potential (E_{cor}) is plotted way below compared with the established E of other metal coupons tested. In addition, among the metals tested, the low carbon steel had the highest current density absorbance and plotted along the lowest potential zone. This suggests that it is the most active metal and the most probable to have the highest corrosion rate. If this will be plotted in the Pourbaix diagram with hydrogen as standard electrode (Fig. 3), it will plot on a region below the lower stability limit which indicates that continuous uniform corrosion is likely to occur. Moreover, its passivation zone is not clearly established and is not vertical but rather sloping. This suggests that given this type of media, the material will have difficulty in forming passive corrosion products that will serve as protective coating as the potential increases. Based on the observations during actual experimental run, the low C steel easily corrodes. Reddish-brown deposits were formed immediately on the surface of the coupons and the test media also turned reddish-brown.

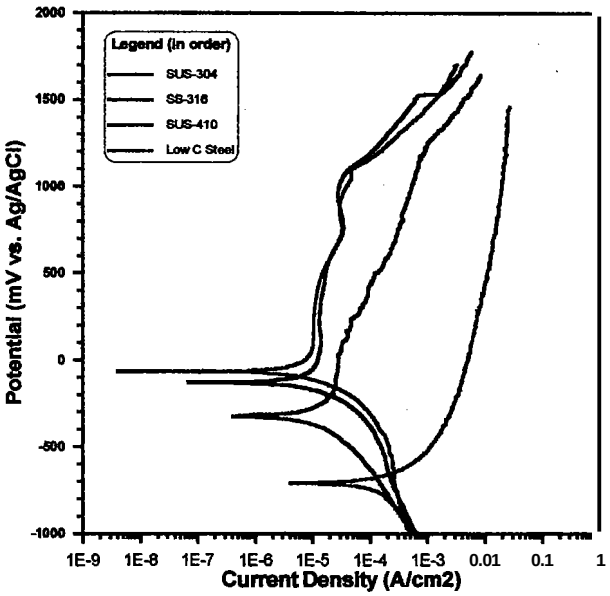

Figure 5. Actual polarization curves of test coupons.

The observed passivation potential of SUS-410 (12% Cr) coupon was so narrow (-130 mV to 32 mV). Above this potential, the protective film is destroyed, making way far the corrosion to proceed at specific rates. During the experiment, from the oxidation potential of +32 mV up, pitting corrosion started to occur which suggests that this metal is also susceptible to corrosion. Both stainless steels SUS-304 and SUS-316 showed an almost identical resistance towards this fluid. However, SUS-304 plots to be more resistant than SUS-316. This is because of the unavailability of new SUS-316 metal coupon. The one used in the experiment have some dents which may have affected the resistance readings. Nevertheless, both coupons showed that it is more resistant and both have the highest ability to develop a very strong passive film as indicated by its wide range of vertical passivation curve.

Table 3. Composition of metal coupons tested by polarization.

Material Tested	Chemical composition (%)										
	C	Si	Mn	P	S	Ni	Cr	Mo	Cu	N	Others
LCS (IF)	0.002	0.01	0.13	0.004	0.004	-	-	-	-	0.003	-
SUS-410	0.15	1.00	1.00	0.04	0.030	-	11.50 ~ 13.5	-	-	-	-
SUS-304	0.08	1.00	2.00	0.045	0.030	8.00 ~ 10.50	18.00~ 20.0	-	-	-	-
SUS-316	0.08	1.00	2.00	0.045	0.030	10.00 ~ 14.0	16.00 ~ 18.0	2.00 ~ 3.00	-	-	-

Table 4. Chemistry of the Upper hi condensate used as electrolyte during l

Sample		COMPOSITION (mg/kg)							
	PH	CO_{2T}	HCO_3	B	Cl	SiO_2	SO_4	NH_3	H_2S
UM-Cond.	5.48	188.1	24.9	4.31	1.83	0.22	<1.0	13.9	21.2
		Na	K	Ca	Mg	Li	Rb	Cs	Fe
		0.07	0.54	0.99	1.55	<0.003	<0.003	<0.002	0.58

Corrosion rates *can* **also** be calculated fiom the polarization curves through graphical method by finding the intersect of the Tafel slope **with** the projected E, The corresponding i_{cor} at this intersecting point (Figure 4) *can* be used to determine the corrosion rates through the modified Faradays law equation (Pound et **al.,** 1984):

$$CR = (I_{cor}*M)/zAF\rho \quad (1)$$

where CR is the corrosion rate (mm/yr), I is the corrosion current (A), M is the molar mass of metal (g/mole), A is area of electrode (mm^2), z is number of electrons transferred per metal atom, F is the Faraday's constant and ρ is the density of metal (g/mm3). But i_{cor}, the current density, is **equal** to current applied per unit area of coupon. Therefore the above equation *can* be rewritten as:

$$CR = (i_{cor}*M)/zF\rho \quad (2)$$

Listed in Table 5, are the E, i_{cor} and the CR of the metals tested. Based on this theoretical calculation of corrosion rates fiom its polarization curves, low carbon steel corrosion rate is 52.5 times higher compared to SUS-304 while SUS-410 is 1.9 times higher compared to SUS-304. Note that this experiment was conducted at static laboratory condition. If these will be coupled with **an** erosive velocity at dynamic condition, these will increase several times higher. Given a 0.2 mm/yr. acceptance criteria for pipeline corrosion rate, low carbon steel is indeed unacceptable. Thus, a more resistant material is needed to handle this fluid i.e. SUS-304 and SUS-316.

Table 5. Calculated corrosion rates fkom the polarization experiment.

Material Tested	E_{cor}	I_{cor}	Corrosion Rate
SUS-304	-62 mV	4.4 E-7 A/cm2	0.04 mm/yr.
SUS-316	-128 mV	4.4 E-7 A/cm2	0.04 mm/yr.
SUS-410	-325 mV	8.2 E-7 A/cm2	0.075 mm/yr.
Low C Steel (IF)	-710 mV	2.3 E-5 A/cm2	2.10 mm/yr.

SUS410 (12% Cr) **as** a martensitic steel, is usually used for turbine blading. However, during the polarization experiment, the polarization curve of ordinary martensitic steel (12%Cr) suggests that it is not reliably resistant to corrosion using the above fluid. Thus, it is concluded that the material of this kind is not appropriate material for Upper Mahiao high **and** low temperature turbine application. To lengthen the life of the turbine while minimizing the rehabilitation cost, is to replace the first two stages parts with a more resistant martensitic steel such **as** 17-4 PH alloy (17%Cr with 4% Mo) *or* its equivalent. In addition, anti-corrosion measures such **as** Continuous backheating should be implemented in order to protect the other turbine parts such as casing and shaft.

Based on the result of the experiments of other researchers such as Lichti **et al.** (1984); Kurata **et al.** (1995); and Sanada **et al. (1998),** they established that martensitic steel with higher percentage of Cr are resistant to **this** type of environment. These types of steels will become more resistant if it will be alloyed with little amount of Ni and **or Mo.** In the case of Mitsubishi, they utilize the 17-4 PH alloy (17% Cr and 4% Mo precipative hardening alloy) in its first and **last** stage blades. Moreover, they use steelite **as** lining on the blade tip to minimize the effect of erosion in the **first** and last stage blades. This alloy and method of putting a protective lining were proven to resist erosion and corrosion induced by **this** kind of steam based on the experience fiom the **nearby** Tongonan-1 power plant operating since 1983 with **almost** similar steam composition with Upper Mahiao. Therefore, material of this kind is ideal **for** Upper Mahiao application.

However, careful yield strength consideration **must** be exercised in the selection **process** of the **material** since the higher the %Cr the alloy tends to become more stronger. But the stronger it **becomes,** the more it is susceptible to **stress** corrosion cracking.

6.0 FUTURE CONDENSATE DISPOSAL

Aside fiom using austenitic stainless steel as condensate line for its disposal. The disposal scheme of the condensates should not be done by direct injection to the reinjection well **smce** it will pose potential damage to the low carbon steel wellbore. The disposal therefore should be done by other **ways** such **as** mixing the condensates with the reinjection brine **prior** to disposal at a ratio not potentially hazardous to field operations **or** by dosing an inhibitor/neutralizing agent. The latter **still needs** several testing **and** maybe a costly option. **Thus,** the **former** was recommended since it is least costly.

Although, the mixing of low temperature condensates (50-60°C) with hot brine (160-180°C) will cause a significant drop in brine temperature, this case will not pose potential scale deposition problem since the acidity of the condensates will act as a pH modifier making the brine pH to go down. This inhibits the silica scale deposition in the pipeline (Weres et al, 1981 and Hirowatari 1988). Moreover, the brine will be diluted minimizing further the tendency to develop silica deposition. In addition, the dissolved components of the brine will buffer the acidity of the dissolve components of the condensate. Corrosion will no longer be a threat to the low carbon steel reinjection pipeline and wellbore.

7.0 CQNCLUSIONS AND RECOMMENDATIONS

- The chemistry of the condensate is corrosive to the existing low carbon steel pipeline.
- Field material testing results have concluded that low carbon steel is not resistant to the acidity brought about by this condensates saturated with dissolved CO_2 and H_2S gases. It further concludes that either SUS-304 and SUS-316, is the ideal alloy for use to handle the condensate fluid disposal for a lifelong utilization.
- Chemical modeling through stability (Pourbaix) diagram also suggests that this fluid will favor the formation of free corrosion products Fe^{++} making a continuous uniform corrosion along the line.
- The polarization curve of the low carbon steel showed that it is incapable of forming a protective layer. It also suggests a continued breakdown of the protective film.
- The analysis of the corrosion samples using SEM, EPMA, XRD and X-Ray Fluorescence analyses showed that there are two distinct layers of corrosion along the low carbon steel line. The lower layer is that of pyrite (FeS_2). While, the upper layer is that of $FeSO_4.H_2O$. This hydrated ferrous sulfate corrosion is the product formed when H_2S reacts with steel aided with the atmospheric oxygen that encrusted into the line forming SO_4. Thus, it is recommended that to mitigate this corrosion problem, austenitic stainless steels should be used since these have a wide range of passivation zones during the polarization experiment.
- Future condensate disposal will be done by mixing it with reinjection brine to avoid borehole corrosion.
- The polarization experiment using SUS 410 (12%Cr martensitic steel) however, showed that it is still susceptible to corrosion. Thus, a more resistant martensitic stainless steel is needed for Upper Mahiao high and low temperature application.
- Martensitic steel with higher percentage of Cr are resistant to this type of environment. These will become more resistant if it will be alloyed with a little amount of Ni and or Mo. This material is ideal for Upper Mahiao application.

REFERENCES

Borshevska, M. K.A. Lichti and P.T. Wilson, 1984. The Relationship Between Corrosion Products and Corrosion Rates in Geothermal Steam. Proceedings, The 6th New Zealand Geothermal Workshop, p. 191.

Forte, N., 1996. The 125 MW Upper Mahiao Geothermal Power Plant, "The Largest Geothermal steam/binary Combined Cycle Plant Starts-Up". Transactions, Vol. 20, p. 743-748.

Hibara, Y. and M. Tahara, 1986. How to Maintain Geothermal Steam Turbines. Proceedings, ASME/IEEE Power Generation Conference, Portland, Oregon.

Hirowatari, K.,1988. Removal and Preventive Methods of Scale Deposition in Geothermal Power Stations. Chinetsu, v.25, No. 4, p. 37-38.

Kurata, **Y.,N.** Sanada, ,H Nanjo, J. Ikeuchi and **K.A.** Lichti, 1995. Material Damage in **A** Volcanic Environment. Proceedings, World **Geothermal** Congress, p. 2409-2413.

Lichti, K.,A., S. **Soylemezoglu** and K.D. Cunliffe, 1980. Geothermal Corrosion and Corrosion Products. Proceedings, The 2nd **New** Zealand Geothermal **Workshop, p.** 103-108.

Lichti, K.A., S.J. Schwann, S.P. White, N.Sanada, **Y. Kurata,** H. Nanjo, J. Ikeuchi and **B.W.Christenson,** 1997. Corrosion in Volcanic Gases. Proceedings, NEDO International Geothermal Symposium, p. 154.

Mashall, T. and W.R. Braithwaite, 1973. Corrosion Control in Geothermal **Systems.** Unesco, 1973. **Geothermal** Energy (Earth Sciences, Vol. 12), p. 151-158.

Mitsubishi **Heavy** Industries, Ltd, 1989. Geothermal Power Generation. Reprinted 1993.

Pound, B.G., M.H. Abdurrahman, M.P. Glucina, RM. Sharp and G.A. **Wright,** 1979. The Measurement of Corrosion Rates of carbon Steel **m** Geothermal Media by the Polarization Resistance Technique.. Proceedings, The 2nd New Zealand Geothermal **Workshop,** p. 97-100.

Romanov, V.V., 1969. Corrosion of Materials: Methods **of** Investigation. Translated from Russian (Israel Program for Scientific Translation), **p.** 115- 156.

Salonga, N.D., RR Villa, RG. Arones, 1998. Disposal Management of Steam Condensates **fiom** a 125 MW Direct Condensation Power Plant Upper Mahiao, Leyte, Philippines. Transactions, Vol. 22 pp. 223-227.

Salonga, N.D., RR Villa, **S.G.** Ramos and M.C. Magdadaro, 1998. Pipeline Corrosion in Condensate Solution Containing Carbon Dioxide and Hydrogen Sulfide **Upper** Mahiao Sector, **Leyte, Philippines.** PNOC-EDC Internal **Report.**

Sanada, N., **Y. Kurata,** H. Nanjo and J. Ikeuchi,1995. Material Damage in **High** Velocity Acidic Fluids. Transactions, Geothermal Resource Council Vol. 19, **pp** 359-363.

Uhlig, **HH** and RW. Revie, 1985. Corrosion and Corrosion Control ***An*** Introduction to Corrosion Science **and** Engineering, 3rd Edition, John Wiley and **Sons.**

Villa, RR. and N.D. Salonga, 1997. UMPP STG-20 **Turbine** Scales and Corrosion Documentation. PNOC-EDC Internal Report.

Villa, RR, N.D. Salonga and J.B. Rosell, 1997. Materials Corrosion Testing in Upper Mahiao Steamlines, Leyte, Philippines. PNOC-EDC Internal Report.

Weres, O., ***Yee,*** A. and Sao, L., 1981. Kinetics of Silica Polymerization, J. Colloid and Inter. F. ***Science.***